The Topographic Impact on Surface Solar Radiation over Taiwan

Yen-Jen Lai[1], Ming-Dah Chou[2] and Po-Hsiung Lin[2]
[1]Experimental Forest, National Taiwan University, Nantou, Taiwan
[2]Department of Atmospheric Sciences, National Taiwan University, Taipei, Taiwan

Abstract

In a mountainous region, the surface slope, orientation (i.e. aspect), and surrounding terrains have a strong impact on the surface *SW* radiation. Taiwan is a subtropical island with complex terrains. The Central Mountain Range extends from north to south of the island. There are numerous rivers with deep valleys emanating from central mountain regions to reach the east and west coasts within a short distance. The island is mostly hills and mountains.

Topographic impact on the surface solar (or shortwave, *SW*) radiation was investigated using a 40-*m* high resolution digital topographic data and a radiative transfer model. With applications to the complex terrain of Taiwan, we found that the spatial variation of the surface *SW* radiation has a strong diurnal cycle. We developed a parameterization of the topographic impact on the surface *SW* radiation that scales the *SW* radiation computed for a flat surface without shading by surrounding terrains. The scaling is separately applied to the direct and diffuse radiation. It is applicable to all clear, aerosol-laden, and cloudy conditions and to all spatial resolutions with $\Delta x > 40$ *m*.

1. Introduction

Surface solar (shortwave, *SW*) radiation is the energy source for all life forms. It affects hydrology, ecology, soil temperature, and climate. Thus, most weather stations have radiometers measuring *SW* radiation for various studies. However, the cost of installation and maintenance of such instruments is enormous, and those measurements can only be made at certain stations instead of covering a large area, such as an entire watershed in complex terrains. Furthermore, a land model or an atmospheric model requires frequent calculations of surface *SW* radiation averaged over a model grid box, which is generally different from point measurements in complex terrains. Therefore, it is important to understand the magnitude of the topographic effect on the surface *SW* radiation and to develop an efficient method for calculating the surface *SW* radiation in complex terrains.

In a mountainous region, the surface slope, orientation (i.e. aspect), and surrounding terrains have a strong impact on the surface *SW* radiation. With the development of Geographic Information System (GIS) and the availability of high-speed computers, efficient methods were developed for calculations of terrain parameters and the surface *SW* radiation over vast mountainous regions [e.g., Dozier and Frew, 1990; Dubayah, 1994; Rich et. al., 1994; Kumar, et al., 1997; Fu and Rich, 2000; Lai, 2003].

The objectives of this study were to determine the degree of the topographic impact on the surface SW radiation and to develop a general scheme for efficiently computing the surface SW radiation in mountainous regions.

2. Datasources

We used the 40–*m* high resolution DEM of the Taiwanese Forestry Bureau (TFB) to investigate the impact of terrain on the surface *SW* radiation over Taiwan. The TFB derived the elevation of each 40–m pixel by applying a stereo-mapping technology to airplane photographical observations. It has a vertical resolution of 1 *m*. Sinks and peaks among pixels are common errors in a DEM. These errors were corrected in this study. Based on the elevation of the DEM pixels, we computed the slope and aspect of the terrain.

3. Methodology

3.1 SW radiative transfer model

The surface *SW* radiation was computed using the National Aeronautics and Space Administration (NASA) CLIRAD-*SW* radiative transfer scheme [Chou and Lee, 1996; Chou and Suarez, 1999]. For calculations of the incoming *SW* radiation at the top of the atmosphere, we need information on the solar constant, the earth-sun distance, and the solar zenith angle (*SZA*). We used a solar constant of 1367 Wm^{-2} in this study. Calculations of the annual variation of the earth-sun distance followed the work of Duffie and Beckman [1980]. The solar declination angle as a function of Julian day was calculated following Cooper [1969]. The *SZA* and solar azimuth angle (*SAA*) can be calculated according to the solar declination, latitude and hour angle by the equation of spherical triangle [Tseng, 1988].

Influenced by the East Asian winter and summer monsoons, as well as the high central mountains, the climate of Taiwan can be grouped into 5 regimes; north vs. south and east vs. west. In calculating the surface *SW* radiation for a given month, we used a single set of monthly-mean temperature and humidity profiles for each of the five climatic regimes. These monthly-mean temperature and humidity profiles were derived from radiosonde observations at the weather sites of the Taiwanese Central Weather Bureau and the Air Force located in those climate regimes. The surface *SW* radiation is not sensitive to ozone. We used a single ozone vertical profile typical of a middle latitude region in radiation calculations.

Solar radiation incident at the Earth's surface or canopies include direct radiation, sky (diffuse) radiation, and the radiation due to reflection by surrounding terrains. The last component is small except over high reflective snow and desert surfaces [Iqbal, 1983; Dingman, 1994]. Over the subtropical mountainous terrain of Taiwan, the surface is mostly covered by low-reflection vegetation, and the incident *SW* radiation originated from the reflection by neighboring land surfaces was ignored in this study.

3.2 Terrain shading

Due to the complex high terrain of Taiwan mountain ranges, the terrain shading of *SW* radiation is expected to be significant. With the 40-*m* high resolution DEM of Taiwan topography, the zenith angle of shading at a given geographical location in a given azimuth angle can be easily computed. The shading angle, H, is defined as the maximum zenith angle that the *SW* radiation is not blocked by surrounding terrains. Larger than this angle, the *SW* radiation is blocked by surrounding terrains. For a grid box located at x_o with an altitude z_o, the shading angle $H_i(\phi)$ in the azimuth direction ϕ due to a grid box located at x_i with an altitude z_i, is give by

$$H_i(\phi) = \tan^{-1}\left(\frac{x_i - x_o}{z_i - z_o}\right) \qquad (1)$$

When the height of all of the grid boxes in the direction ϕ is considered, the shading angle is then the minimum of $H_i(\phi)$ for all x_i.

3.3 Direct *SW* radiation

For a surface with a slope angle of β oriented in the azimuth angle ϕ_n (i.e. the aspect) measuring clockwise from the north, the angle between the sun beam and the normal of the sloped surface θ_T is given by

$$\cos\theta_T = \sin\beta\sin\theta_o\cos(\phi_o - \phi_n) + \cos\beta\cos\theta_o \qquad (2)$$

where θ_o and ϕ_o are the *SZA* and *SAA*, respectively. When the incident *SW* radiation is >90° from the normal of the irradiated surface, the radiation is blocked by the sloped surface causing "self-shading".

In numerical land and atmospheric models, a model domain is divided into grid boxes. Radiative fluxes are computed for each grid box. Since the ratio of the area of a sloped surface in a given grid box to the horizontal area of the grid box (i.e. grid size) is $1/\cos\beta$, the direct *SW* radiation incident at the sloped surface *in terms of an unit area of the horizontal surface* in a grid box, B_t, is then

$$B_t = \left(\frac{B_h}{\cos\beta}\right)\left(\frac{\cos\theta_T}{\cos\theta_o}\right) \qquad (3)$$

where B_h is the direct *SW* radiation incident at a flat surface unobstructed by surrounding terrains. Solar radiation is blocked by surrounding terrains if $\theta_o > H(\phi_o)$ or due to self-shading if $\theta_T > 90°$.

3.4 Diffuse *SW* radiation

For a horizontal surface unobstructed by surrounding terrains, the downward sky (diffuse) radiation is given by

$$F_h = \left(\int_{\phi=\pi/2}^{3\pi/2} d\phi \int_{\theta=0}^{\pi/2} I(\theta,\phi)\cos\theta\sin\theta\, d\theta + \int_{\phi=-\pi/2}^{\pi/2} d\phi \int_{\theta=0}^{\pi/2} I(\theta,\phi)\cos\theta\sin\theta\, d\theta\right) \qquad (4)$$

where I is the intensity, θ is the zenith angle, and ϕ is the azimuth angle of the incident radiation. For isotropic radiation, $F_h = \pi I$.

When a surface is tilted with a slope $\tan^{-1}\beta$ oriented in the azimuth direction ϕ_n and shaded by surrounding terrains, the isotropic downward radiation *per unit area of the tilted surface* is given by

$$F_t = \frac{F_h}{\pi\cos\beta}\left(\int_{\phi-\phi_n=\pi/2}^{3\pi/2} d(\phi-\phi_n) \int_{\theta_T=0}^{\gamma_1} \cos\theta_T \sin\theta_T d\theta_T + \int_{\phi-\phi_n=-\pi/2}^{\pi/2} d(\phi-\phi_n) \int_{\theta_T=0}^{\gamma_2} \cos\theta_T \sin\theta_T d\theta_T\right) \qquad (5)$$

where θ_T is the angle between the incident radiation and the normal of the sloped surface given by Equation (2) except the angles (θ_o, ϕ_o) are replaced by (θ, ϕ), and γ_1 and γ_2 are given by

$$\gamma_1 = Min\left[H(\phi-\phi_n) + \lambda, \frac{\pi}{2}\right]$$
$$\gamma_2 = Max\left[H(\phi-\phi_n) - \lambda, 0\right] \qquad (6)$$

and $\lambda(\phi-\phi_n, \beta)$ is the tilt angle of the surface in the azimuth direction $\phi-\phi_n$ given by

$$\lambda(\phi-\phi_n, \beta) = \tan^{-1}\left[\tan\beta\cos(\phi-\phi_n)\right] \qquad (7)$$

This tilt angle is β for $\phi = \phi_n$ and 0 for $\phi - \phi_n = -\pi/2$ and $+\pi/2$. It is noticed that λ is positive for $-\pi/2 < \phi - \phi_n < \pi/2$ and negative for $\pi/2 < \phi - \phi_n < 3\pi/2$.

In deriving Equation (5), we assumed that the diffuse radiation is isotropic. This assumption is generally valid except for the cases of thin cirrus clouds and dust aerosols, which have particles with irregular shapes. Calculations of anisotropic radiation require models that can resolve scattering in all directions. Since the directional sky radiation is a function of the SZA and the optical properties of clouds and dusts, it would add another layer of complexity in studies on the topographic impact on the SW radiation if the anisotropic sky radiation is to be resolved. However, calculations for some sample cases with anisotropic sky radiation will provide useful information on the degree that anisotropic sky radiation affects the surface diffuse radiation. This is an interesting topic and will be a future research plan.

In a land or an atmospheric model, the surface SW radiation is computed assuming a flat surface without terrain shading. The downward diffuse SW radiation is equivalent to that given by Equation (4). Since the area of a tilted surface is $1/\cos\beta$ times the area of a flat surface, the insolation *per unit area with respect to the horizontal surface* of a grid box, F_t, is given by

$$F_t = V\left(\frac{F_h}{\cos\beta}\right) \tag{8}$$

where V is the effect on the diffuse radiation due to both terrain and self shading. For an isotropic diffuse radiation,

$$V = \frac{1}{\pi}\left(\int_{\phi-\phi_n=\pi/2}^{3\pi/2} d(\phi-\phi_n)\int_{\theta_T=0}^{\gamma_1}\cos\theta_T\sin\theta_T d\theta_T + \int_{\phi-\phi_n=-\pi/2}^{\pi/2} d(\phi-\phi_n)\int_{\theta_T=0}^{\gamma_2}\cos\theta_T\sin\theta_T d\theta_T\right) \tag{9}$$

The value of V is between 0 and 1. It is noticed that the topographic factor defined above is similar to the sky-view factor defined in some previous studies [e.g, Dozier and Frew, 1990; Lai, 2003]. Figure 1 shows the frequency distribution of V for the 40-m resolution terrain of Taiwan. It has a mean value of 0.90 and a standard deviation of 0.096. For the 40-m resolution of grid boxes, 23.3% of the land over Taiwan is flat and unobstructed by surrounding terrains, i.e. V=1.0. However, there is an extreme case of deep valley where the shading is drastic with V = 0.11.

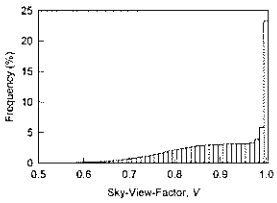

Figure 1. The frequency distribution of sky-view factor, V, for the 40-m resolution terrain of Taiwan.

4. Implications for SW radiation calculations in land and atmospheric models

4.1. Temporal distributions of domain-mean *SW* radiation

In this subsection we investigate the diurnal and annual variations of the domain-mean *SW* radiation with all of the topographic effects included.

Figure 2a shows the diurnal variation of domain-mean total (direct + diffuse) *SW* radiation throughout a year. The diurnal variation is shown as a function of normalized local time, *NLT*, ranging from 0 at dawn, to 0.5 at noon, and to 1.0 at dusk. Figure 2b is the same as Figure 2a, except the *SW* radiation is shown as a function of the cosine of the solar zenith angle, μ_o, instead of *NLT*.

The domain-mean *SW* radiation, $\overline{f}$, attains a maximum at local noon, *NLT* = 0.5, and decreases nearly symmetrically with *LT* deviating from noon toward dawn and dusk (Figure 2a). At noon, the maximum *SW* radiation decreases from summer solstice to winter solstice in accordance with the increase of noontime *SZA*. Over a large region such as the entire Taiwan area, the mean *SW* radiation should depend only on *SZA* but not the slope and shading of terrains. This is shown in Figure 2b that the *SW* is nearly constant for a given μ_o. However, the *SW* radiation is slightly smaller on the summer solstice than the winter solstice due to a greater Earth-Sun distance on the summer solstice.

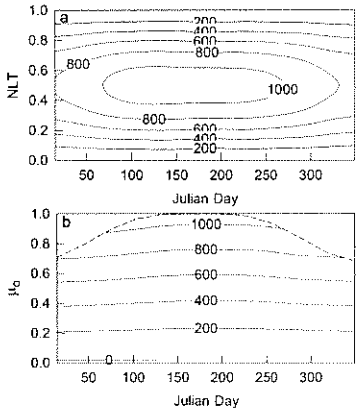

Figure 2. Diurnal-annual distribution of the domain-mean total (direct + diffuse) *SW* radiation in terms of the normalize local time, *NLT* (top panel, a) and the cosine of the solar zenith angle, μ_o (bottom panel, b). Units: Wm^{-2}.

Figure 3a shows the standard deviation, σ_f, of the 40-*m* resolution total *SW* radiation over Taiwan. The pattern of the temporal distribution of σ_f shown in Figure 3a is quite similar to that of $\overline{f}$ as shown in Figure 2a. However, the maximum σ_f (the 300-Wm^{-2} contour lines) occurs in mid-morning and mid-afternoon in June and July (Julian days 150-210) but spreads over a long span of the day from mid-morning to mid-afternoon in December and January. Just as $\overline{f}$ shown in Figure 2a, this pattern is also controlled by *SZA*. Figure 3b shows that the maximum σ_f occurs when $\mu_o \sim 0.55$, or $SZA \sim 55°$. For a large μ_o, the *SZA* is small, and so is the effect of terrain shading, which leads to a small σ_f. For a small μ_o, on the other hand, the incoming *SW* radiation is small, which also leads to a small σ_f. For *SZA* in the range 50-60°, σ_f reaches 300 Wm^{-2}, and the ratio $\sigma_f / \overline{f}$ is >0.5.

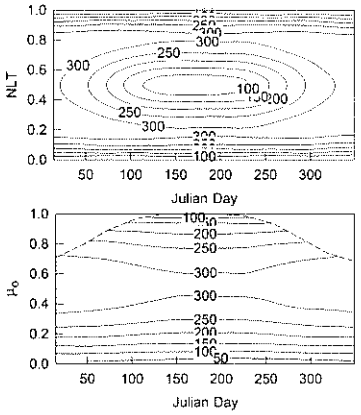

Figure 3. Same as Figure 2, except for the standard deviation, σ_f, of the surface *SW* radiation.

4.2. Impact of spatial resolution on daily-mean *SW* radiation

The impact of topography on the surface *SW* radiation decreases as the size of grid boxes increases, i.e. a degraded horizontal resolution. For the case with spatially homogeneous incoming *SW* radiation at the surface, the topography, except altitude, should have little impact on the surface *SW* when averaged over a large region. In such a case, shading and slope of the surface can be ignored in calculating the surface *SW* radiation. The threshold size of a grid box, which is the lower limit of the grid-box size that the slope and shading effects can be neglected in *SW* radiation calculations, is dependent upon the complexity of topography. The more complex is the topography, the larger the threshold size.

Figure 4 shows the standard deviation of the daily mean *SW* radiation, σ_F, over Taiwan as a function of spatial resolution for the 15th of June and December. It is shown as a percentage of the domain-mean *SW* radiation, $\overline{F}$. For each of the degraded grid box with a size of Δx, the aspect, shading angle, and sky-view factor were computed using the 40-*m* DEM data based on the scheme mentioned in Section 3.

For the December case shown in Figure f, $\sigma_F / \overline{F}$ decreases nearly exponentially for $\Delta x < 2$ *km* and remains nearly constant for $\Delta x > 5$ *km*. It decreases from 44 % for $\Delta x = 40$ *m* to 9 % for $\Delta x = 5$ *km*, and remains nearly unchanged for $\Delta x > 10$ *km*. The results demonstrate that, throughout the entire year, the effects of slope and terrain shading on the surface *SW* radiation are insignificant for a region larger than 5 *km*.

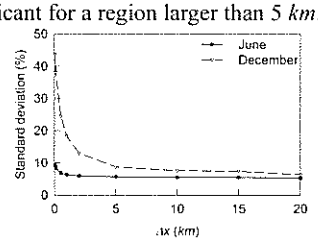

Figure 4. Standard deviation of the spatial distribution of surface *SW* radiation over Taiwan, σ_F, as a function of the spatial resolution, Δx. The standard deviation is normalized with the domain-mean *SW* radiation, which is ~367 Wm^{-2} in June and 210 Wm^{-2} in December.

4.3. Scaling of surface *SW* radiation

A radiation scheme in an atmospheric model normally computes direct and sky (diffuse) *SW* radiation incident at a flat surface without obstruction by surrounding terrains. These quantities are equivalent to B_h and F_h. When considering the effect of topography, the direct and diffuse *SW* radiation can be computed by scaling B_t and F_t using Equations (3) and (8). Nearly without exceptions, the size of a grid box, Δx, in an atmospheric model is much greater than 40 *m*, and the mean direct radiation of a large grid box can be derived from Equation (3) and expressed as

$$\overline{B_t}(\Delta x) = \kappa \overline{B_h}(\Delta x) \tag{9}$$

where $\overline{B_h}$ is the mean direct radiation of the coarse grid box with a horizontal surface unobstructed by surrounding terrains,

$$\overline{B_h}(\Delta x) = \frac{1}{m}\sum_{j=1}^{m} B_{h,j}(\Delta x_n) \tag{10}$$

the scaling factor κ for topographic effects is given by

$$\kappa(\theta_o,\phi_o)=\left[\frac{1}{m}\sum_{j=1}^{m}\frac{B_{h,j}(\Delta x_o)}{\cos\beta_j}\frac{\cos\theta_{T,j}}{\cos\theta_o}\right]/\overline{B_h}(\Delta x) \quad (11)$$

the subscript j is the index for a 40-m grid box, the subscript m denotes the total number of 40-m grid boxes in a spatially degraded grid box, and $\Delta x_o = 40\ m$.

Similarly, the mean diffuse radiation of a large grid box can be derived from Equation (8) and expressed as

$$\overline{F}_t(\Delta x)=\chi\overline{F}_h(\Delta x) \quad (12)$$

where $\overline{F}_h$ is the mean diffuse radiation of the coarse grid box with a flat surface unobstructed by surrounding terrains,

$$\overline{F_h}(\Delta x)=\frac{1}{m}\sum_{j=1}^{m}F_{h,j}(\Delta x_o) \quad (13)$$

and the scaling factor χ for topographic effects is given by

$$\chi=\frac{1}{m}\sum_{j=1}^{m}\left(\frac{V_jF_{h,j}}{\cos\beta_j}\right)/\overline{F_h}(\Delta x) \quad (14)$$

In deriving the sky-view factor V, we assumed that the diffuse radiation was isotropic, and χ is independent of *SZA* and *SAA*. For a fixed grid size, Δx, in an atmospheric model, the scaling factor χ is only a function of the location of the grid box, x, whereas the scaling factor κ is a three-dimensional function of θ_o, ϕ_o, and x.

For the *SW* radiation within a coarse grid box, e.g. $\Delta x = 5\ km$, variations of sub-grid *SW* radiation for flat and unobstructed surfaces, $B_{h,j}$ and $F_{h,j}$, are small, and Equations (18) and (21) reduce to

$$\kappa(\theta_o,\phi_o)=\frac{1}{m\cos\theta_o}\sum_{j=1}^{m}\frac{\cos\theta_{T,j}}{\cos\beta_j} \quad (15)$$

$$\chi=\frac{1}{m}\sum_{j=1}^{m}\left(\frac{V_j}{\cos\beta_j}\right) \quad (16)$$

Equivalent to Equations (16) and (19), the incident surface *SW* radiation, F, can now be written as

$$F_{dir}(\Delta x)=\kappa(\theta_o,\phi_o)R_{dir}(\Delta x) \quad (17)$$

$$F_{dif}(\Delta x)=\chi R_{dif}(\Delta x) \quad (18)$$

where R is the low spatial-resolution radiation incident at a flat unobstructed surface computed using a radiative transfer model, and the subscripts *dir* and *dif* denote, respectively, the direct and diffuse radiation.

For each of the 40-m DEM grid boxes over Taiwan, we computed a single value of χ and a two dimensional array of $\kappa(\theta_o,\phi_o)$ with resolutions of $\Delta\theta_o = 5^\circ$ and $\Delta\phi_o = 10^\circ$. They were computed only once and saved as pre-computed tables. The low resolution box-mean κ and χ were then derived from Equations (22) and (23). The scaling factor χ includes the effect of slope on the area of land surface, $1/\cos\beta$. Different from the sky-view factor V, values of χ can be greater than 1. It is noted that the only assumption applied in the derivation of V is isotropic sky radiation. Therefore, the scaling of Equations (24) and (25) are applicable to all clear, cloudy, and aerosol-laden skies. Figure 5 shows the frequency distribution of χ over Taiwan for $\Delta x = 1\ km$ and $5\ km$. The topographic impact on the diffuse *SW* radiation is important for $\Delta x = 1\ km$ and only marginally important for $\Delta x = 5\ km$.

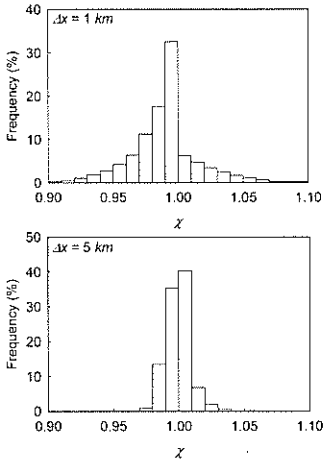

Figure 5. The frequency distributions of χ over Taiwan for Δx=1 *km* (top panel) and 5 *km* (bottom panel).

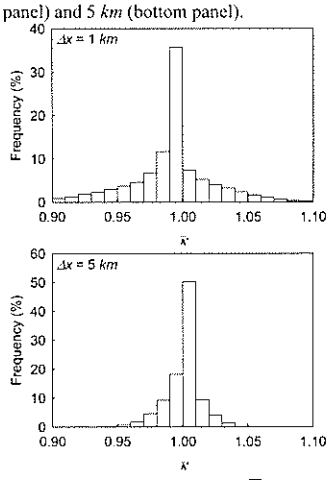

Figure 6. The frequency distribution of $\overline{\kappa}$ over Taiwan for Δx=1 *km* (top panel) and 5 *km* (bottom panel)computed for 22 June.

Since the incoming *SW* radiation varies with θ_o, the daily mean value of κ can be approximated by

$$\overline{\kappa}=\frac{\sum_t\kappa(t)\mu(t)}{\sum_t\mu(t)} \quad (19)$$

where $\mu = \cos(\theta_0)$. The $\overline{\kappa}$ is then the daily mean impact of topography on the direct *SW* radiation, which is a

function of Julian day and the location of a spatially degraded box. Figure 6 shows the frequency distribution of $\overline{\kappa}$ over Taiwan on the summer solstice, 22 June, for Δx = 1 *km* and 5 *km*. Similar to the diffuse *SW* radiation, it shows that the topographic impact on the surface direct *SW* radiation is important for Δx = 1 *km* and marginally important for Δx = 5 *km*.

5. Conclusion

Spatial variations of the surface *SW* radiation are large in mountainous regions. We used the complex terrain of Taiwan as an example to study the impact of topography on the surface *SW* radiation. Based on the 40-*m* high resolution DEM of Taiwanese Forestry Bureau, we derived the mean surface height, slope, and terrain shading for various sizes of grid boxes (Δx). Spatial and temporal variations of the surface *SW* radiation were then computed using the Goddard CLIRAD *SW* radiation model for various spatial resolutions ranging from 40 *m* to tens of *km*. Results show that the spatial variation of surface *SW* radiation has a strong diurnal variation and depends greatly on the size of grid boxes. The standard deviation, σ_f, of the surface *SW* radiation over Taiwan is nearly constant for a given *SZA*. The maximum σ_f occurs at *SZA*~55°, which corresponds to mid-morning (early morning) and mid-afternoon (late afternoon) in winter (summer). The topographic impact on the spatial variation of the *SW* radiation also strongly depends on spatial resolution. The standard deviation of daily-mean *SW* radiation, σ_F, in winter decreases rapidly with increasing size of grid boxes for Δx < 5 *km*. For Δx > 5 *km*, σ_F is small and stays nearly constant. In summer, the topographic impact on the daily-mean surface radiation is much weaker than in winter.

We developed a scheme for parameterization of the topographic impact on the surface *SW* radiation. The parameterization scales the surface *SW* radiation computed using a radiative transfer model that assumes a flat surface without shading by surrounding terrains. The scaling factors were derived based on the 40-*m* high resolution topography and were separately applied to direct and diffuse *SW* radiation. The scaling for the direct *SW* radiation is a function of location and solar zenith and azimuth angles, whereas the scaling for the diffuse *SW* radiation is a function only of location. The scaling scheme can be applied to all clear, aerosol-laden, and cloudy conditions.

Acknowledgments. The work of Y.-J. Lai was supported by the Experimental Forest, National Taiwan University, Taiwan (grant no. 95B08 and 97A07), and the work of M.-D. Chou and P.-H. Lin was supported by the National Science Council, Taiwan.

References

Chou, M.-D., and K.. Lee (1996), Parameterizations for the absorption of solar radiation by water vapor and ozone, J. Atmos. Sci., 53, 1203-1208.

Chou, M.-D., and M. J. Suarez (1999), A shortwave radiation parameterization for atmospheric studies, Technical Report Series on Global Modeling and Data Assimilation, 15, pp. 1-42, NASA/TM-1999-104606.

Cooper, P. I. (1969), The absorption of *SW* radiation in solar stills, Solar Energy, 12, 333-346.

Dingman, S. L. (1994), *Physical hydrology*, 575 pp., Macmillan Publishing Co., New York.

Dozier, J., and J. Frew (1990), Rapid calculation of terrain parameters for radiation modeling from digital elevation data, IEEE Transactions on Geoscience and Remote Sensing, 28(5), 963-969.

Dubayah, R. C. (1994), Modeling a *SW* radiation topoclimatology for the Rio Grande River Basin, J. Veg. Sci., 5, 627-640.

Duffie, J. A., and W. A. Beckman (1980), *Solar Engineering of Thermal Processes*, 762 pp., Wiley, New York.

Fu, P., and P.M. Rich (2002), A geometric solar radiation model with applications in agriculture and forestry, Computers and Electronics in Agriculture, 37, 25-35.

Iqbal, M. (1983), *An introduction to SW radiation*, 390 pp., Academic Press, Toronto Ont.

Lai, Y.J. (2003), The study on estimating temporal-spatial distribution of solar irradiance in watershed, Ph.D. thesis, 125 pp., National Taiwan Univ., Taiwan. [in Chinese with English summary]

Kumar, L., A.K. Skidmore and E. Knowles (1997), Modeling topographic variation in solar radiation in a GIS environment, International Journal of Geographical Information Science, 11(5), 475-497.

Rich, P. M., R. Dubayah, W.A. Hetrick, and S.C. Saving (1994), Using Viewshed models to calculate intercepted solar radiation: applications in ecology, American Society for Photogrammetry and Remote Sensing Technical Papers, pp. 524–529.

Tseng, C.Y. (1988), *Atmospheric Radiation*, pp.63~77, Linking Publishing Co., Taiwan